stellarator news

An international journal of news from the stellarator community

Editor: James A. Rome Issue 167 October 2019
E-Mail: James.Rome@stelnews.info Phone: +1 (865) 482-5643
On the Web at https://stelnews.info

Enhancement of Energetic-ion Confinement Study Using Comprehensive Neutron Diagnostics in LHD

In a fusion reactor, a burning plasma is sustained by alpha particle heating [1]. Therefore, energetic ion confinement has been intensively studied to predict the confinement of alpha particles in a burning plasma. In the Large Helical Device (LHD), energetic particle confinement has been studied using neutral beam (NB) injection [2–4]. In a hydrogen plasma regime, study of energetic ion confinement has been mainly studied primarily by measuring charge-exchange of energetic particles using a neutral particle analyzer (NPA), as well as escaping energetic particles using fast ion loss detection (FILD) [5–7]. Studies of magnetohydrodynamic (MHD) mode-induced beam ion transport/loss have also been reported [8–14]. In LHD, operation with deuterium gas was initiated in March 2017 [15]. One of the goals of the deuterium plasma campaign in LHD was the expansion of energetic particle studies. A predictive study based on numerical simulation using the steady-state Fokker-Planck model showed that the beam-thermal neutrons should be dominant [15]. Therefore, by means of neutron diagnostics, we can obtain information regarding energetic particles confined inside the plasma.

Comprehensive Neutron Diagnostics Installed in LHD

Neutron diagnostics such as the ex-vessel neutron flux monitor (NFM) [16–19] in order to measure total neutron emission rate S_n, the neutron activation system (NAS) [20] to perform shot-integrated measurement of DD and secondary DT neutron yields, the vertical neutron camera (VNC) [21–24] to obtain the radial profile of neutron emission, and scintillating-fiber (Sci-Fi) detectors [25–26] to conduct time-resolved measurements of DT neutron yield have been developed and installed to enhance energetic particle study in LHD, in addition to radiation safety management. The commissioning of those diagnostics is reported in Refs. 27–31.

Global Confinement of Beam Ions

Study of S_n on NB-heated plasmas has been performed for various magnetic axis positions (R_{ax}) in LHD. Beam-thermal and beam-beam reaction fractions were evaluated in the case of balanced NB injection. Time-resolved analysis of thermal, beam-thermal, and beam-beam fractions was performed by the TASK/FP code [32, 33]. It is confirmed that the beam-thermal component is dominant, as pre-

In this issue . . .

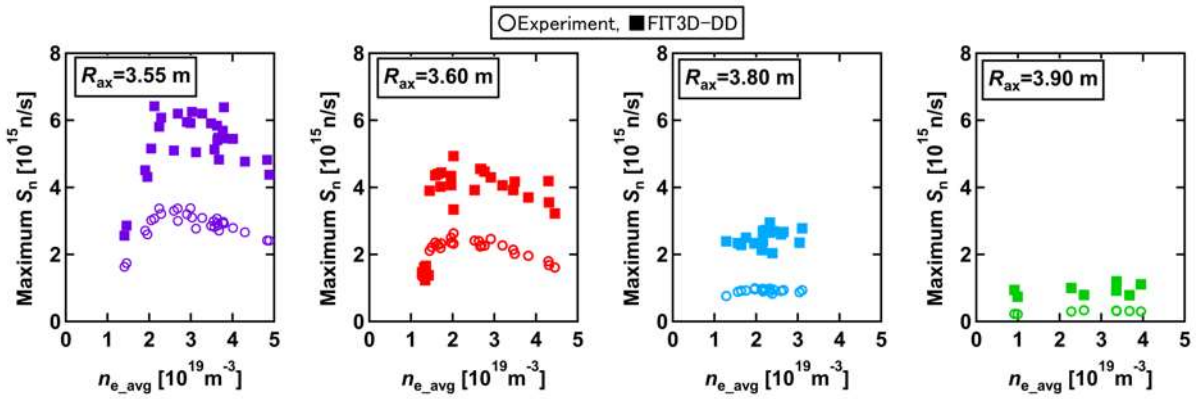

Fig. 1. Electron density dependence of total neutron emission rate S_n for R_{ax} from 3.55 m to 3.90 m.

dicted by Ref. 15. The beam-beam component accounts for approximately 1/5 of S_n. The relatively high beam-beam fraction is due to balanced NB injection. S_n dependence on electron density was surveyed. Figure 1 shows the dependence of the maximum S_n on n_{e_avg} with R_{ax} of 3.55 m to 3.90 m. As the Fokker-Planck model predicted [15], the maximum S_n has a peak at n_{e_avg} of around 2.5×10^{19} m^{-3}. Maximum S_n decreases with outward shift of R_{ax} at the same density. To understand S_n dependence on R_{ax} and n_{e_avg}, the beam-thermal neutron emission rate was calculated by using the FIT3D-DD code [34]. The dependence of S_n on n_{e_avg} is successfully reproduced though S_n was overestimated by almost two times in FIT3D-DD, but the shape of the curve is in rough agreement to experiment.

Fusion Gain

The equivalent fusion gain in DT plasma Q_{DT} has been studied in N-NB heated plasmas. The ratio of fusion gain in DD plasma Q_{DD} on equivalent Q_{DT} were evaluated using the FBURN code [35]. Maximum Q_{DT}/Q_{DD} of 249 is obtained in the case of deuterium NB injection into a triton plasma. The maximum equivalent Q_{DT} reached 0.11 (Fig. 2(a)), which is comparable with that in large tokamaks with 5 MW NB injection [36–38]. It is found that the equivalent Q_{DT} linearly increases with $T_{e0}^{1.5}$ [Fig. 2(b)]. When beam-thermal neutrons are dominant, equivalent Q_{DT} can be expressed as equivalent $Q_{DT} \sim S_n/P_{NB} \sim n_i \times P_{NB} \times \tau_s/P_{NB} \sim n_i \times T_e^{1.5}/n_e \sim T_e^{1.5}$. The plot shown in Fig. 2(b) is consistent with fusion reaction origin.

NB Blip Experiments

Blip experiments with total neutron emission measurements were performed to study beam ion confinement in an MHD-quiescent plasma heated by positive-ion-source-based NB (P-NB) injection (two beamlines with beam energies of 60-80 keV).

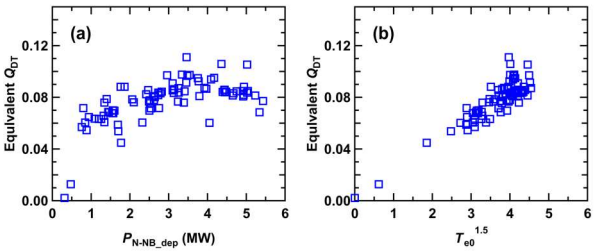

Fig. 2. Dependence of equivalent Q_{DT} on (a) NB deposition power and (b) $T_{e0}^{1.5}$. Equivalent Q_{DT} reached 0.11.

A short-pulse P-NB having a pulse width of 20 ms is injected into the electron-cyclotron-heated plasma [Fig. 3(a)]. A rapid increase in S_n is observed due to P-NB injection. The characteristics of slowing down and transport of beam ions appear in the S_n decay state after the P-NB is turned off. The decay time of S_n obtained in experimentally is 215 ms. To understand beam ion transport and loss, Global NEoclassical Transport (GNET) simulation [39] and the FBURN simulation without radial diffusion have been performed (Fig. 3(b)). We obtained almost the same rise time for S_n in the experiment, FBURN calculation, and GNET calculation. We also have obtained a relatively short decay time for S_n with GNET (216 ms)

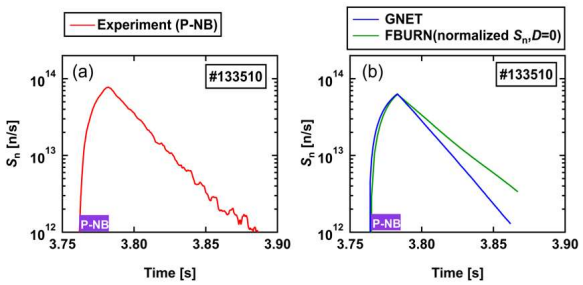

Fig. 3. Time evolution of S_n in P-NB blip (a) in experiment and (b) calculated by GNET and FBURN.

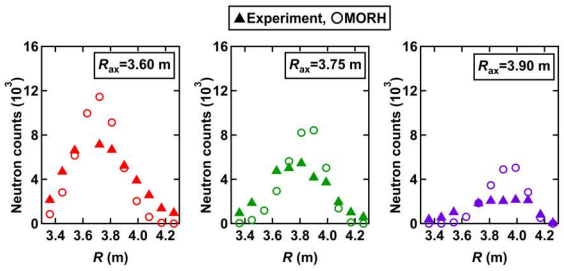

Fig. 4. Line-integrated neutron emission profile obtained for R_{ax} of 3.60 m, 3.75 m, and 3.90 m by experiment and MORH simulation.

compared with that calculated by FBURN (250 ms). It is found that GNET can reproduce the time trace of S_nn. Hence, we can describe the transport of NB blip beam ions in the low-β MHD quiescent plasma using neoclassical models.

Radial Profile of Neutron Emission

Neutron emission profiles in plasmas heated with negative-ion-source-based NBs (N-NB) (3 beamlines with beam energy 180 keV) were measured using a vertical neutron camera (VNC) in various R_{ax} conditions. The time trace of neutron counts shows that the counts are higher in the central channel than in the edge channel. Line-integrated neutron emission profiles at t of 3.7 s to 4.3 s in three R_{ax} configurations are plotted in Fig. 4. Due to the increase in S_n with the inward shift of R_{ax}, as shown in Fig. 1, neutron counts of VNC increase accordingly. The position of peak neutron counts is shifted according to R_{ax}. We also have calculated the line-integrated neutron profile using numerical simulation with the MORH code [40] based on HINT equilibrium [41] with an effective charge of 1 assumed. Figure 4 also shows the line-integrated neutron profiles in three different R_{ax} configurations calculated by MORH. Although we have obtained two times higher neutron counts than that obtained in the experiment, the simulation reproduces the shift in neutron count peak according to R_{ax} position.

Triton Burnup Experiment

A triton burnup experiment has been conducted for the first time in stellarator/heliotron devices. The study of 1-MeV triton burnup can be regarded as a proxy for DT born alpha particle confinement. We installed Sci-Fi detectors in order to measure the secondary DT neutron emission. We used the triton burnup ratio, defined as total DT neutron emission yield divided by total DD neutron emission yield, in order to show the MeV confinement capability [42–49]. Typical time traces from the triton burnup experiment show that there are two decay components in S_n after the NB is turned off. The fast component and the

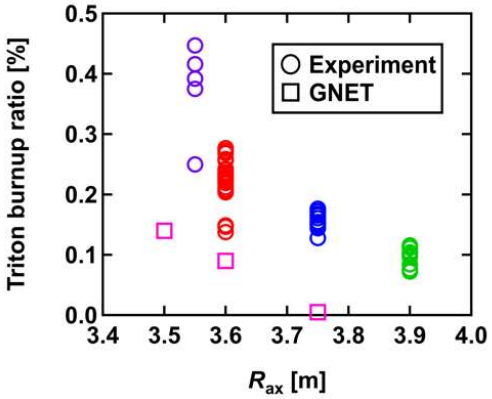

Fig. 5. Triton burnup ratio dependence on R_{ax} obtained in experiment and GNET simulation.

slow component correspond to DD and DT neutrons, respectively. The time trace of the relatively slow component matches the DT neutron rate measured by a Sci-Fi detector. The dependence of the triton burnup ratio on R_{ax} is plotted in Fig. 5. The result shows that we obtained a higher triton burnup ratio in the small R_{ax} case than in the large R_{ax} case. We achieved a triton burnup ratio of 0.45%. The LHD record is a similar value to that obtained in tokamaks such as ASDEX Upgrade and KSTAR [48, 49] whose minor radius is comparable to that of LHD. Figure 5 shows the triton burnup ratio evaluated using GNET. The GNET result also shows the larger triton burnup ratio in the the inward-shifted configuration. The lower triton burnup ratio in GNET may be due to re-entering effects because in GNET, the triton orbit is calculated in Boozer coordinates.

Summary

Energetic particle confinement research in stellarator/heliotron devices is benefiting from the deuterium LHD plasma experiments. The dependence of S_n on electron density shows the same trend as predicted by numerical simulations. The beam-beam components account for 20% of S_n in N-NB-heated plasmas as shown by TASK/FP code. We have achieved equivalent Q_{DT} of 0.11, which is almost the same value obtained in large tokamaks with the same NB heating power. A short NB injection experiment into an MHD-quiescent plasma shows that the time evolution of S_n can be described by neoclassical models. Neutron emission profile measurement and triton burnup experiments were performed for the first time in stellarators and helical devices. The peak of the line-integrated neutron profile measured by VNC shifted according to R_{ax}. The triton burnup ratio increases with the inward shift of R_{ax}, as expected on the basis of numerical simulation, and reaches 0.45%.

References

[1] Fasoli, A. et al., 2007 Nucl. Fusion **47** S264.

[2] Osakabe M. et al., 2010 Fusion Sci. Technol. **58** 131.

[3] Toi, K. et al., 2010 Fusion Sci. Technol. **58** 186.

[4] Toi, K. et al., 2011 Plasma Phys. Controlled Fusion **53** 024008.

[5] Isobe, M. et al., 2010 Fusion Sci. Technol. **58** 426.

[6] Ogawa, K. et al., 2008 Plasma Fusion Res. **3** S1082.

[7] Ogawa, K. et al., 2009 Journal of Plasma Fusion Res. SERIES **8** 655.

[8] Osakabe, M. et al., 2006 Nucl. Fusion **46** S911.

[9] Ogawa, K. et al., 2010 Nucl. Fusion **50** 084005.

[10] Isobe, M. et al., 2010 Contrib. Plasma Phys. **50** 540.

[11] Ogawa, K. et al., 2012 Plasma Science and Technology **14** 269.

[12] Ogawa, K. et al., 2012 Nucl. Fusion **52** 094013.

[13] Ogawa, K. et al., 2013 Nucl. Fusion **53** 053012.

[14] Ogawa ,K. et al., 2014 Plasma Phys. Controlled Fusion **56** 094005.

[15] Osakabe, M. et al., 2017 Fusion Sci. Technol. **72** 199.

[16] Isobe, M. et al., 2014 Rev. Sci. Instrum. **85** 11E114.

[17] Nakano, Y. et al., 2014 Rev. Sci. Instrum. **85** 11E116.

[18] Nakano, Y. et al., 2014 Plasma Fusion Res. **9** 3405141.

[19] Nishitani, T. et al., 2017 Fusion Eng. Des. **123** 1020.

[20] Pu, N. et al., 2017 Rev. Sci. Instrum. **88** 113302.

[21] Ogawa, K. et al., 2014 Rev. Sci. Instrum. **85** 11E110.

[22] Uchida, Y. et al., 2014 Rev. Sci. Instrum. **85** 11E118.

[23] Uchida, Y. et al., 2017 Rev. Sci. Instrum. **88** 083504.

[24] Ogawa, K. et al., 2018 Rev. Sci. Instrum. **89** 095010.

[25] Takada, E. et al., 2016 Plasma Fusion Res. **11** 2405020.

[26] Takada, E. et al., 2019 Rev. Sci. Instrum. **90** 043503.

[27] Isobe, M. et al., 2018 IEEE Transactions on Plasma Science **46** 2050.

[28] Isobe, M. et al., 2018 Nuclear Fusion **58** 082004.

[29] Ogawa, K et al., 2017 Plasma Fusion Res. **12** 1202036.

[30] Ogawa, K et al., 2018 Nucl.r Fusion **58** 034002.

[31] Ogawa, K. et al., 2018 Nucl. Fusion **58** 044001.

[32] Nuga, H. and Fukuyama, A. 2011 Prog. in Nucl. Sci. Technol. **2** 78

[33] Nuga, H. et al., 2019 Nucl. Fusion **59** 016007.

[34] Murakami S. et al., 1995 Trans. Fusion Tech. **27** 256.

[35] Ogawa, K. et al., 2018 Plasma Phys. Controlled Fusion **60** 9.

[36] Jassby, D. L. et al., 1991 Phys. Fluids B: Plasma Phys. **3** 2308.

[37] Keilhacker, M. and the JET Team, 1990 Phys. Fluids B: Plasma Phys. **2** 1291.

[38] Nishitani, T. et al., 1994 Nucl. Fusion **34** 1069.

[39] Murakami, S. et al., 2002 Nucl. Fusion **42** L19.

[40] Seki, R. et al 2015 Plasma Fusion Res. **10** 1402077.

[41] Suzuki, Y. et al., 2003 Plasma Phys. Controlled Fusion **45** 971.

[42] Barnes, C. W. et al., 1998 Nucl. Fusion **38** 597.

[43] Källne, J. et al., 1988 Nucl. Fusion **28** 1291.

[44] Hoek, M. et al., 1996 Nucl. Instrum. Methods Phys. Res. A **368** 804.

[45] Heidbrink, W. W., Chrien, R. E., and Strachan, J. D., 1983 Nucl. Fusion **23** 917.

[46] Duong, H. and Heidbrink, W. W., 1993 Nucl. Fusion **33** 211.

[47] Batistoni, P. et al., 1987 Nucl. Fusion **27** 1040.

[48] Hoek, M., Bosch, H. S. and Ullrich, W., 1999 "Triton burnup measurement at ASDEX Upgrade by neutron foil activation," IPP-Report IPP-1/320.

[49] Jo, J. et al., 2016 Rev. Sci. Instrum. **87** 11D828.

[50] Reichert, S., Nature Phys. **15**, 622 (2019); Ogawa, K., et al., 2019 Nucl. Fusion **59** 076017.

Mitsutaka Isobe and Kunihiro Ogawa
National Intitute for Fusion Science
Toki, Japan
E-mail: kogawa@nifs.ac.jp

Plans for EPOS: A Tabletop-sized, Superconducting, Optimized Stellarator For Matter/antimatter Pair Plasmas

Why make a plasma out of electrons and positrons?

The large mass asymmetry between positive and negative species is a cornerstone of the physics of traditional electron/ion plasmas. It is not surprising, then, that quasineutral plasmas comprising positively and negatively charged particles of identical mass ("pair plasmas") are expected to exhibit a number of properties qualitatively different from those of electron/ion plasmas. Without the inherent separation of time scales and length scales that arises from the large mass ratio, many standard plasma physics phenomena vanish — e.g., sheaths, Faraday rotation, whistler waves, and lower hybrid waves. To consider pair plasmas necessitates rederiving plasma physics from the ground up, a project that theory and simulation first began to tackle more than 40 years ago [1] and that to date has resulted in hundreds of predictions. Among these, for example, are changes to the physics of reconnection, soliton solutions, and turbulence; in certain regimes and magnetic configurations, pair plasmas are expected to exhibit "remarkable stability" to anomalous transport modes that tend to dominate electron/ion plasmas [2].

Studying plasmas with reduced mass ratios is a way to improve our understanding of "normal" plasmas, e.g., in such aspects such as reconnection and tokamak heat fluxes [3]. Testing predictions of how plasma physics changes in the limit of a mass ratio of unity will thus confirm our understanding of fundamental aspects of plasma phenomena, validating our ability to simulate plasmas in various regimes. This study will also improve our knowledge of our universe, in which pair plasmas dominated for 1–10 seconds after the Big Bang (a period known as the Lepton Era), and in which electron-positron plasmas are still being generated (e.g., in the neighborhood of pulsars and active galactic nuclei). Hence, there is a compelling need for experiments to complement the ever-growing body of theoretical/computational literature about pair plasmas, which can be thought of as the "hydrogen atom of plasma physics" (i.e., a comparatively simple system that nevertheless informs understanding of its far more complex cousins).

Electron/positron plasmas, which can be magnetized easily, are of particular interest, and there has recently been significant progress in experimental methods to study them in the laboratory—a significant experimental challenge to which there are several approaches that span a range of target densities, temperatures, and confinement times. Among these is the approach (Fig. 1) of the APEX (A Positron Electron eXperiment) collaboration [4], which is bringing together people, expertise, and experimental hardware from the Max Planck Institute for Plasma Physics (IPP, where the project is based) and universities in Germany, the United States, and Japan. APEX has been has making strides toward its goal of magnetically confining a cold electron/positron pair plasma in a dipole magnetic field, recently demonstrating proof-of-principle results in the areas of lossless injection across flux surfaces and subsequent long confinement of injected positrons [5]. In parallel with the next steps of development of existing programs (positron beam optimization, positron pulse accumulation, and the construction of the levitated dipole trap), a new branch of the collaboration's experimental program will be launched at the end of this year, involving the design, construction, and operation of a second magnetic confinement device for the pair plasma: a stellarator.

As shown in Fig. 1, the final configuration for the APEX collaboration will bring together a world-class positron beam (from the NEPOMUC NEutron-induced POsitron source MUniCh); a series of Penning-Malmberg-type traps to collect the steady-state NEPOMUC beam into pulses, then combine these pulses as non-neutral positron plasmas in ever greater numbers; and two complementary toroidal traps (APEX and EPOS) in which the positrons will be confined with electrons to make the pair plasmas.

How to make a plasma out of electrons and positrons

In order to create an electron/positron pair plasma in the laboratory, one first needs access to sufficient amounts of antimatter (which, needless to say, is notoriously hard to come by). Specifically, for a plasma with a temperature of 0.1–5 eV in a volume of 5–50 liters (a tabletop device), between 10^9 and 10^{11} positrons are required to achieve 10 Debye lengths—i.e., the classic threshold above which a collection of charged particles constitutes a "plasma," as defined by the relevance of collective forces in comparison to individual particles' kinetic energies [4, 9].

These conditions can be reached using a world-class e^+ beam that can produce up to 10^9 e^+/s [6], plus a series of non-neutral plasma traps to accumulate the steady-state beam into cool, dense, tailorable pulses [7]. Finally, the positrons need to be combined with a comparable number of electrons; this is best done in a magnetic trap that provides excellent confinement for both positive and negative species, either for fully quasineutral plasmas or for non-neutral plasmas, without requiring plasma current (which these extremely low-density plasmas would not to be able to generate). Two obvious choices are a levitated dipole trap and an optimized stellarator. Although they have in

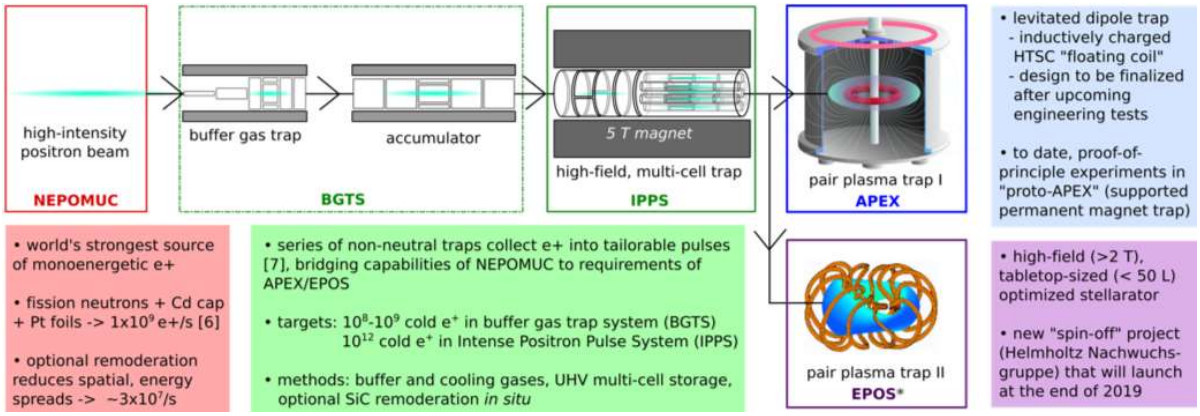

Fig. 1. The final configuration for the APEX collaboration will bring together a world-class positron beam (from the NEutron-induced POsitron source MUniCh); a series of Penning-Malmberg-type traps to collect the steady-state NEPOMUC beam into pulses, then combine these pulses as non-neutral positron plasmas in ever-greater numbers; and two complementary toroidal traps (APEX and EPOS) in which the positrons will be confined with electrons to make the pair plasmas. (*Note: Since EPOS hasn't been designed yet, this is a placeholder image, borrowed from Ref. [8].)

common that they both meet the requirements described above, the plasma physics in these two configurations tends to be very different, due to the disparate magnetic field topologies (Table 1); they have complementary technical strengths and weaknesses, as well. Comparing the behavior of pair plasmas in the APEX dipole (with axisymmetry and strong flux expansion) to those with approximately the same parameters in the EPOS stellarator (with magnetic shear and long connection lengths) can be expected to deeply enrich the findings of both.

Naturally, one of the first questions that comes up when discussing a matter/antimatter pair plasma is, “Won't it just annihilate?” There are indeed several different channels through which this will occur, and each has a well-known cross section that can be used to determine how long the plasma would persist if that were the limiting factor [10]. For pair plasmas in the target density and tem-

Stellarator	Levitated dipole
Steady state	Steady state on typical plasma time scales
Fusion relevance	Astrophysical relevance
Negligible flux expansion	Strong flux expansion
Irrational as well as rational flux surfaces	Each B-field line closes after one pass
Long B-field connection lengths	Short B-field connection lengths
parallel force balance counteracts instabilities	Parallel force balance does not counteract instabilities
drift orbit confinement requires optimization	Drift orbits always confined (due to axisymmetry)
Passing particles most easily confined	Passing particles most sensitive to departures from axisymmetry
Indefinite operation with permanently attached electrical and thermal contacts	Inductive charging, cooling/warming cycles, repeated making/breaking of thermal contacts
Many 3D coils	2-3 planar coils (floating, lifting, charging)
Requires positron pulses for fueling	Possibility for steady-state fueling, using inward transport processes unique to dipoles

Table 1. A stellarator and a levitated dipole have very different and complementary physics, as well as different technical advantages and disadvantages.

perature ranges, these all come out to lifetimes longer than a day. Although annihilation is not therefore expected to limit plasma lifetime, it will still provide a tool for diagnosing the plasma (especially when enhanced by gas or pellet injection) [5].

Preliminary design/optimization considerations

The design and optimization for EPOS will start in earnest in a couple of months, but it is abundantly clear from the outset that it will be very different from that for a fusion reactor:

- ⇨ Small device size (between 5 and 50 liters) but strong magnetic fields (>2 T, so as to be able to take advantage of cyclotron cooling, a valuable tool in non-neutral plasma physics experiments).
- ⇨ Low temperatures (0.1–5 eV) and extremely low densities (10^{11}–10^{13} m^{-3}).
- ⇨ Debye length > Larmor radius.
- ⇨ Very far from the regime of MHD.
- ⇨ No ions (except when deliberately introduced).
- ⇨ No pressure, divertor, heat loads, or neutrons.
- ⇨ Significant flexibility with respect to the design of the coils/current sheets.

Nevertheless, the EPOS experiment will be provide a meaningful test bed for next-generation stellarator design tools that are also used for fusion, in particular with an eye toward maximizing construction tolerances [11]—something that is especially important for a small device—and minimizing neoclassical transport. Because low-density pair plasmas are predicted to be turbulence-free in well-chosen geometries [2,12], and because quasi-neutral pair plasmas will have zero ambipolar field due to mass symmetry, thereby eliminating the effect of "orbit healing" due to radial electric fields, EPOS can explore the upper bounds of what neoclassical optimization can provide—albeit in a system with different types of collisions than a fusion plasma. Positrons also provide an extremely sensitive probe for where and when charged particles are lost.

From the engineering side, high-temperature superconductors (HTSCs) are an attractive option for their ability to provide higher fields while relaxing the cooling requirements, but it must first be assessed whether they would demand overly restrictive constraints on the bending radii of the coils/wires. Like UST-2 [13], EPOS aims to use 3D-printed winding frames/surfaces. In addition, it will seek to take advantage of new technologies for 3D printing metal structures suitable for UHV conditions and cryogenic cooling.

An avenue will also be needed for getting the positrons into the device from the NEPOMUC beam line. **E**×**B** drift injection has worked extremely well for getting NEPOMUC's positrons into proto-APEX and then trapping them there [5]. In order to use a similar scheme for injecting them into EPOS, a region of "close approach" to the plasma from the e^+ beam line will be needed. In some exploratory designs for stellarator fusion reactors, an extended helical coil has been proposed, in order to create large access ports; in the "stray field" of such a coil could be the right place to hook up the positron beam line.

Looking ahead to pair plasmas

The estimated timeline for EPOS involves spending approximately the first year of the program developing the design of the device, in close collaboration with stellarator optimization experts at IPP and in the Simons "Hidden Symmetries" Collaboration, as well as in consultation with superconducting magnet researchers in Germany and the United States. Construction will start in the second year. In the third year, commissioning will be performed with electrons. This will be followed by installation at NEPOMUC (which is operated at the FRM II neutron source, next door to IPP Garching) and the addition of positrons, leaving approximately three years for electron/positron experiments and cross-comparisons between APEX and EPOS.

As a primary method of diagnosing the positron and pair plasmas, both devices will be taking measurements of the 511 keV gamma rays produced by annihilation events. Several types of gamma ray detection are planned: coincident detection such as that used in positron emission tomography (PET) scans, high-energy-resolution spectroscopy with high-purity Ge detectors, and lower-resolution detection of line- or volume-integrated annihilation rates with scintillator/PMT (photomultiplier tube) assemblies. (Variations on this last technique have been used in proto-APEX to date and worked extremely well, especially when supported with simulations [5].) The information gathered will be then used to calculate important qualities of the pair plasma, such as its density and temperature [4] — thereby allowing us to determine when we have achieved multiple Debye lengths, a key milestone.

The first things to study with the pair plasmas will be the confinement time and stability. If electron/positron plasmas in these devices are indeed uniquely stable, that will be encouraging, since historically the magnetic confinement of plasmas has repeatedly turned out to be more complex than anticipated. But either way, it will be an opportunity to explore a fascinating new frontier in plasma physics.

The EPOS project is jointly funded by the Helmholtz Association and the Max Planck Institute for Plasma Physics, within the framework of the Helmholtz Young Investigator Groups program.

The APEX collaboration receives/has received support from the European Research Council (ERC) under the European Union's Horizon 2020 research and innovation programme; the Deutsche Forschungsgemeinschaft (DFG); the Helmholtz Postdoc Programme; the UC San Diego Foundation; the Japan Society for the Promotion of Science (JSPS); and the National Institute for Fusion Science (NIFS).

References:

[1] V. Tsytovich and C. B. Wharton. Comments Plasma Phys. Controlled Fusion, **4** 91–100 (1978).

[2] P. Helander. Phys. Rev. Lett. **113** 135003 (2014).

[3] A. Le et al., Phys. Rev. Lett. **110** 135004 (2013); N. T. Howard et al., Nucl. Fusion **56** 014004 (2016).

[4] T. Sunn Pedersen et al., New J. Phys. **14** 035010 (2012).

[5] E. V. Stenson et al. Phys. Rev. Lett. **121** 235005 (2018); J. Horn-Stanja et al., Phys. Rev. Lett. **121** 235003 (2018).

[6] C. Hugenschmidt et al., New J. Phys. **14** 055027 (2012).

[7] J. R. Danielson et al., Rev. Mod. Phys. **87** 247 (2015).

[8] P. R. Garabedian and G. B. McFadden, J. Res. Natl. Inst. Stand. Technol. **114** 229 (2009).

[9] E. V. Stenson et al., J. Plasma Phys. **83** 595830106 (2017).

[10] C. J. Crannel et al., Astrophys. J. **210** 582 (1976); R. G. Greaves and C. M. Surko, AIP Conf. Proc. **606** 10 (2002); P. Wallyn et al., Astrophys. J. Supp. Ser. **92** 551 (1993).

[11] J.-F. Lobsien et al., Nucl. Fusion **58** 106013 (2018).

[12] T. Sunn Pedersen et al., Fusion Sci. Technol. **46** 200 (2004).

[13] V. M. Queral, www.fusionvic.org

Eve V. Stenson
Max Planck Institut für Plasmaphysik
Garching, Germany
E-mail evs@ipp.mpg.de